Available online at www.sciencedirect.com
ScienceDirect
Trans. Nonferrous Met. Soc. China 26(2016) 63−73
Transactions of Nonferrous Metals Society of China
www.tnmsc.cn

Influence of rutile (TiO_2) content on wear and microhardness characteristics of aluminium-based hybrid composites synthesized by powder metallurgy

C. ANTONY VASANTHA KUMAR[1], J. SELWIN RAJADURAI[2]

1. Department of Mechanical Engineering, Scad College of Engineering and Technology, Cheranmahadevi, Tirunelveli 627414, Tamilnadu, India;
2. Department of Mechanical Engineering, Government College of Engineering, Tirunelveli 627007, Tamilnadu, India

Received 1 February 2015; accepted 18 June 2015

Abstract: The effect of rutile (TiO_2) content on the wear and microhardness properties of aluminium (Al)-based hybrid composites was explored. The proposed content of TiO_2 (0, 4%, 8%, 12%, mass fraction) was blended to Al−15%SiC composites through powder metallurgy (P/M) process. Wear test was conducted using pin-on-disc apparatus under dry sliding conditions. Fabricated preforms were characterized using X-ray diffractometer (XRD), scanning electron microscope (SEM) and energy-dispersive X-ray spectrometer (EDS). Optical micrographs of the composite preforms display uniform distribution of TiO_2 throughout the matrix. Quantitative results indicate that wear resistance and microhardness increase with the increase of TiO_2 content. SEM images unveil that high wear resistance is attributed to high dislocation density of deformed planes and high hardness of TiO_2. SEM images of wear debris display gradual reduction in mean size of debris when TiO_2 content increases. EDS spectra confirm the presence of oxide layer which obviously reduces the effective area of contact between the sliding surfaces thereby lowers the wear loss of composites. The observation concludes that delamination and adhesive wear are the predominant mechanisms.
Key words: aluminium; metal-matrix composite; rutile; powder metallurgy; sliding wear

1 Introduction

There is a tremendous demand for advanced engineering materials with high strength, light weight, and increased resistance to wear in aerospace, civil and sliding components of automobile sectors. This leads to the development of aluminium matrix composites (AMCs) [1−4]. Aluminium is principally reinforced with hard phases such as SiC, TiC, TiB_2 and Al_2O_3 and soft phases like graphite (Gr) and MoS_2 [5,6]. Recently, extensive study on Al−SiC composites has been made as SiC in particular delivers enhanced wear resistance and mechanical properties [7−17].

The presence of SiC makes the composites hard to be machined due to its brittle property. Addition of metal oxides shifts the brittleness of SiC and widens its engineering applications [18]. Oxide phases extensively improve the fracture toughness of the materials. The application of minerals as potential reinforcements has progressively emerged by considering the environmental aspects. Minerals are environment-friendly, inexpensive and available in abundance which place them to be significant reinforcement materials for the composites [19].

Rutile is a mineral composed predominantly of titanium dioxide (TiO_2). Rutile, a common natural form of TiO_2, is readily available, inexpensive and holds substantial wear resistance, mechanical and thermal properties [19]. RAMESH et al [20] reinforced Al 6061 alloy with TiO_2 and achieved significant enhancement in wear resistance and hardness characteristics. CHAUDHURY et al [21] blended TiO_2 with Al−Mg and the composite showed better wear resistance than the base material. TROMANS and MEECH [22] confirmed that rutile possesses superior physical and engineering properties. Comprehensive survey on various literatures revealed that no detailed findings are available for powder metallurgy (P/M) processed Al−SiC−TiO_2 (rutile) hybrid composites. P/M is widely adapted for achieving uniform distribution of reinforcing phase within the matrix and to produce near net shaped components [23−26].

The present investigation therefore intended to

Corresponding author: C. ANTONY VASANTHA KUMAR; Tel: +91-9489161661; E-mail: findvasanth@gmail.com, anto_vasanth@rediffmail.com
DOI: 10.1016/S1003-6326(16)64089-X

study the impact of TiO_2 (rutile) on the dry sliding wear behavior of Al−15%SiC (mass fraction) composites using P/M. Detailed analysis was made on the dry sliding wear behavior and the microhardness of the proposed material. Interpretation of the worn surface was done using scanning electron microscope (SEM) and energy dispersive X-ray spectrometer (EDS) to uncover the wear mechanism. Wear debris collected during the wear test also indicates the mechanism of sliding wear.

2 Experimental

2.1 Processing of samples

Pure atomized aluminium powders supplied by M/S Metal Powder Corporation, Sivakasi, Tamilnadu, India are preferred as the matrix material. The mean diameter of aluminium particle chosen based on ASTM B−214 is 37 μm. ABJ Shipping and Exports Pvt Ltd, Mumbai, India supplied SiC with an average diameter of 45 μm and Kerala Minerals and Metals Ltd, Kerala, India supplied TiO_2 particles with an average diameter of 44 μm, respectively. Table 1 provides the details of reinforcements used for the present study. SEM images of as-received aluminium, SiC and TiO_2 powders confirmed their particle size (Figs. 1(a)−(c)). To carry through the wear study, the following composites were prepared: 1) Pure Al, 2) Al/15%SiC, 3) Al/15%SiC/4%TiO_2, 4) Al/15%SiC/8%TiO_2, 5) Al/15%SiC/12%TiO_2 (mass fraction).

Table 1 Parameters of reinforcement particles

Reinforcement	Mean diameter of grains/μm	Density/(g·cm^{-3})
SiC	45	3.21
TiO_2 (rutile)	44	4.23

The proposed composite samples were manufactured using powder metallurgy technique. Powders were weighed to the required fractions using an electronic weighing machine having an accuracy level of 0.001 g and mixed uniformly using a planetary mixer with 12 mm-diameter steel balls. Mixing powders with the support of rolling steel balls reduce agglomeration of particles. Effective bonding of reinforcements with the matrix is essential to meet good properties. Hence, the powders were preheated to 200 °C before compaction. Powders were cold compacted at 800 MPa in a uniaxial press. During each run, die wall was kept under manual lubrication using graphite particles. The green compacts were sintered at 650 °C in an electric muffle furnace for 2 h as hinted by YUSUF [26]. The consolidated samples were cooled in the furnace for 8 h. The specimens were then machined to a diameter of 12 mm and a height of 30 mm.

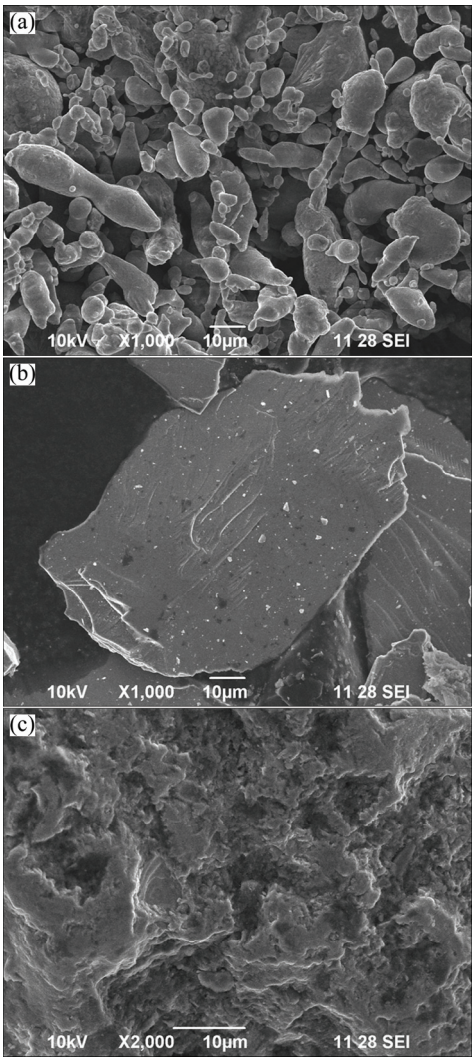

Fig. 1 SEM images of as-received materials: (a) Aluminium powders; (b) SiC particles; (c) TiO_2 (rutile) particles

The base of the cylindrical specimens was polished in two stages through a standard procedure. Initially, rough polishing was carried out on the samples using standard abrasive papers of 400, 1000, 1400, 2200 grits. The composite preforms were then exposed to fine polishing using 1 μm diamond paste. After polishing the specimens, microhardness test was carried out based on ASTM E 384 11e1 using Vickers hardness testing machine (Mitutoyo, Japan). During the test, samples were loaded with 10 N for 10 s. The test was run away at twenty different locations and the mean was computed. Density of the composites was calculated by Archimedes principle. The specimens were weighed using an electronic weighing balance of accuracy 0.001 g.

2.2 Wear test

The dry sliding wear test was conducted using a pin-on-disc equipment (Ducom, Bangalore) at 60 N applied load with ASTM G99−05. Table 2 furnishes the

Table 2 Wear parameters and test conditions employed for study

Material and parameter	Description
Pin material	Al, Al−15%SiC, Al−15%SiC−x%TiO_2 (x=4, 8, 12)
Counter disc material	EN31 steel with hardness of HRC 65
Pin dimensions	Cylinder with diameter of 12 mm and height of 30 mm
Sliding velocity/(m·s^{-1})	0.5, 1, 1.5, 2, 2.5
Sliding distance/m	1000, 1500, 2000, 2500, 3000
Applied load/N	60

wear parameters and the test conditions. The counter disc preferred was EN31 grade steel hardened to HRC 65 ground to 1.6R_a surface roughness. Before proceeding with the test, the cylindrical pins and the counter disc were cleaned with acetone. During sliding wear, debris of the pin material got wedged to the counter face, which was then removed using organic solvents. The mass loss of the pin was evaluated using an electronic weighing balance with an accuracy of 0.001 g. Consecutive six measurements were chosen for each test and the mean of all was considered.

3 Results and discussion

3.1 Metallographic study

The extent of uniformity of reinforcement distribution in the matrix and the grain structure can be observed through microstructural examinations. Microstructural study was made using an optical microscope (QS Metrology, Mumbai, India and Model: JSJL 17).

The predetermined shapes of composites were prepared for microscopic study after polishing through standard procedures. The samples were finely polished using silicon carbide papers of 400, 1000, 1400 and 2200 grits. The mirror-like finishing surface to be examined was then obtained using a 1 μm diamond paste followed by suspension in distilled water. Polished specimens were submitted to an etching process using Keller's reagent and were allowed to settle for 10 s. Figures 2 shows the micrographs of the samples prepared for the

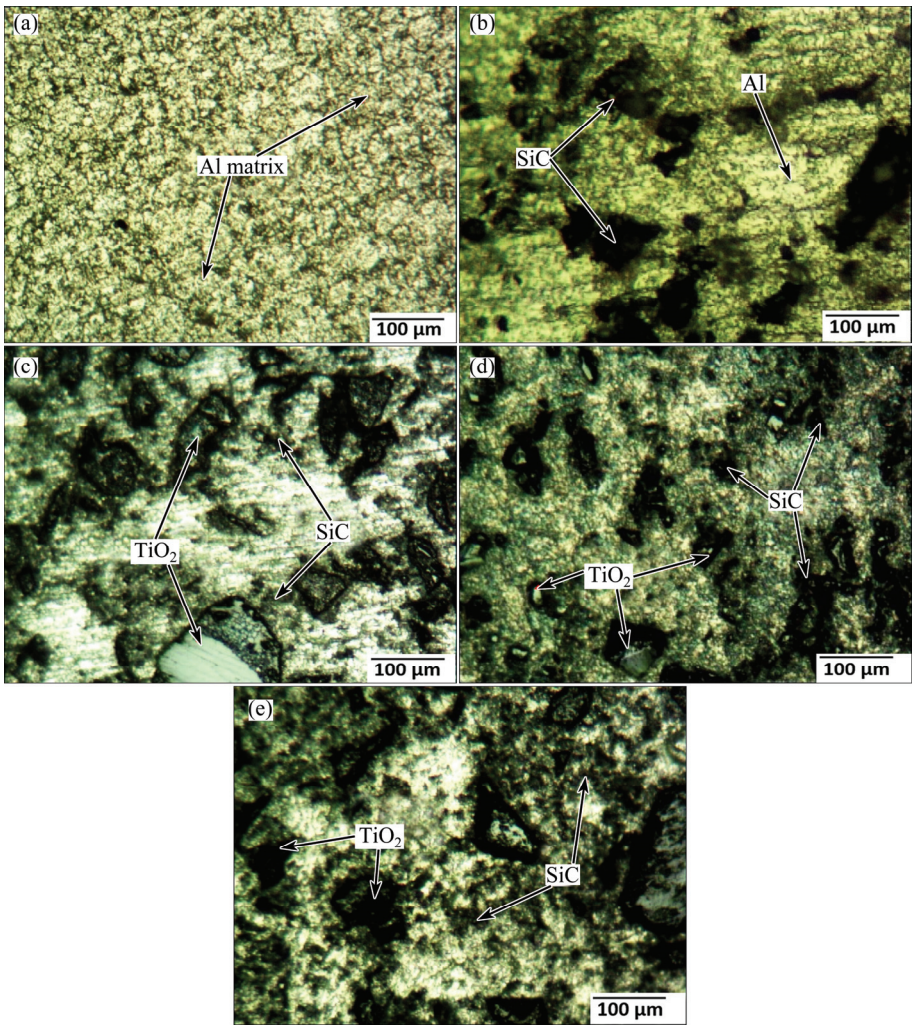

Fig. 2 Optical micrographs of processed samples: (a) Pure Al; (b) Al−15%SiC; (c) Al−15%SiC−4%TiO_2; (d) Al−15%SiC−8%TiO_2; (e) Al−15%SiC−12%TiO_2

proposed Al−SiC−TiO_2 (rutile) hybrid composites. It is apparent from the micrographs that SiC and TiO_2 particles were distributed uniformly throughout the matrix. From the micrographs, it was observed that hard reinforcements of SiC and TiO_2 displayed strong bonding with the Al matrix that further enabled the uniform transfer of load from the matrix to the reinforcements.

3.2 Identification of crystalline compounds

Figure 3 represents the quantitative determination of phases existed in the sintered preforms. The crystalline compounds were identified using Panalytical X'pert Powder X'celerator Diffractometer at Manaonmaniam Sundaranar University, Tirunelveli, Tamilnadu, India. Among the compounds identified, aluminium possessed the strongest peak. The presence of SiC and TiO_2 phases is also evident in the XRD pattern. The XRD patterns confirmed the absence of any intermetallic compounds in the sintered specimen of all compositions.

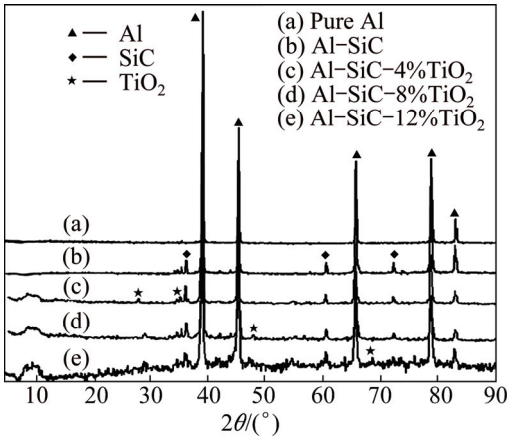

Fig. 3 XRD patterns of Al−SiC−TiO_2 composites with varying contents of TiO_2

3.3 Density and microhardness study

Figure 4 indicates the influence of TiO_2 on the density and microhardness of the proposed hybrid composites. It is eminent that the density and the microhardness increase proportionately with TiO_2 content. When the content of TiO_2 in the matrix increases, dislocation density of composites increases, which resists plastic deformation during sliding. Uniform distribution of the reinforcements in the base matrix and the elevated hardness of TiO_2 also compliment high density and microhardness of the composites.

3.4 Influence of TiO_2 (rutile)

Figure 5(a) shows the change in friction coefficient with the mass fraction of TiO_2. It is found that the friction coefficient increases along with the increase of TiO_2 content. Hybrid composites reinforced with 12% TiO_2 reveal higher friction coefficient than the non-hybridized Al−SiC composites and the base matrix. Increase in friction coefficient is due to high plastic strain developed when adhered particles of reinforcements behave like second body abrasives during sliding wear [27,28].

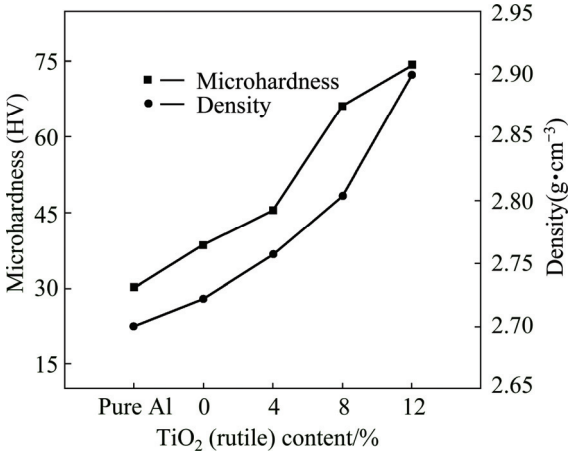

Fig. 4 Density and microhardness of Al−15%SiC− x%TiO_2 composites with content of TiO_2

Hybrid composites reinforced with 4% TiO_2 demonstrated lower coefficient of friction than other compositions (8% and 12% of TiO_2). The oxide layer developed on the worn surface of 4% TiO_2 composite reduces the area of contact between the sliding faces (steel counterface and the face of the composite pin) and lowers the friction coefficient. Figure 5(b) denotes the effect of TiO_2 particulate content on wear loss of Al hybrid composites. Graphical analysis reveals a progressive diminution in the wear loss when the TiO_2 particulate content increases. Figure 5(b) also confirms that the hybridization of TiO_2 to Al−15% SiC composite improves the wear resistance of the composites. Improved wear behaviour of the hybrid composites with the addition of TiO_2 might be explained by its high hardness. High hardness of TiO_2 restricts the plastic flow during sliding wear that leads to reduced wear loss [28]. Better interface bonding between the matrix and the reinforced particles increases the shear strain required to produce plastic flow, which further contributed to the improved wear resistance [29].

3.5 Influence of sliding velocity

Figure 6(a) illustrates the effect of sliding velocity on the friction coefficient of Al hybrid composites. It was noted that at constant sliding distance, the friction coefficient increases as a function of sliding velocity [30]. For any sliding velocity, the friction coefficient gradually increases when the TiO_2 content increases. Furthermore, composites reinforced with TiO_2 show higher coefficient of friction than the unreinforced

Al−15%SiC and the base matrix. The heat developed during the sliding wear oxidizes the surface and a protective oxide layer forms. At high sliding speeds, the micro machining effect of the reinforcement phases breaks down the protective layer, which allows the sliding surfaces to have direct metal-to-metal contact. Direct contact of sliding faces increases the coefficient of friction [31]. Figure 6(b) shows the influence of sliding speed on the wear loss of the proposed hybrid composites. It implies that increase in mass fraction of TiO_2 reduces the wear loss of Al hybrid composites. Hybrid composites reinforced with 12% TiO_2 exhibit high wear resistance during the sliding process. At high sliding velocity, the rate of contact between the counter face and the pin is high. The frequent contact of sliding faces increases the frictional heat, thereby softens the matrix. Subsequent regular contact of sliding faces along with softer matrix leads to more loss of material [32,33].

3.6 Influence of sliding distance

Figure 7(a) shows the disparity of friction coefficient with the sliding distance. The analysis reveals that along with sliding distance, the friction coefficient increases for both Al matrix and hybrid composites [30]. Hybrid composites reinforced with 12% TiO_2 exhibit higher friction coefficient than other composites. Elevated friction coefficient of hybrid composites can be due to the development of plastic strain in particles, as the duration of contact between sliding surfaces increases. High plastic strain promotes localized adhesion of both SiC and TiO_2 particles to the worn surface. Adhered particles form an interface film that contributes to high friction coefficient of the composites [34].

The effect of sliding distance on the wear loss of the proposed hybrid composites is unveiled through Fig. 7(b). The graph shows that for constant sliding velocity, wear losses of both Al matrix and hybrid composites increase with the sliding distance. Nevertheless, at all sliding speeds, hybrid composites reinforced with 12% TiO_2 demonstrate better wear resistance than other composites. Superior hardness possessed by TiO_2 particles supports low wear loss of 12% TiO_2 hybrid composites. During sliding wear, fragmentation of particles takes place when the amount of TiO_2 particulate increases. Fragmentation of particles

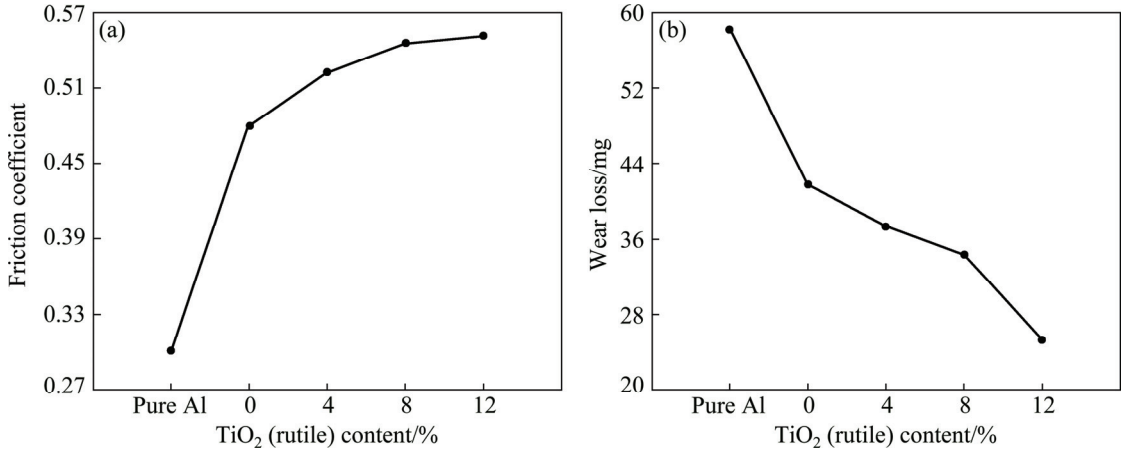

Fig. 5 Effect of TiO_2 (rutile) particulate content on friction coefficient (a) and wear loss (b) of Al hybrid composites

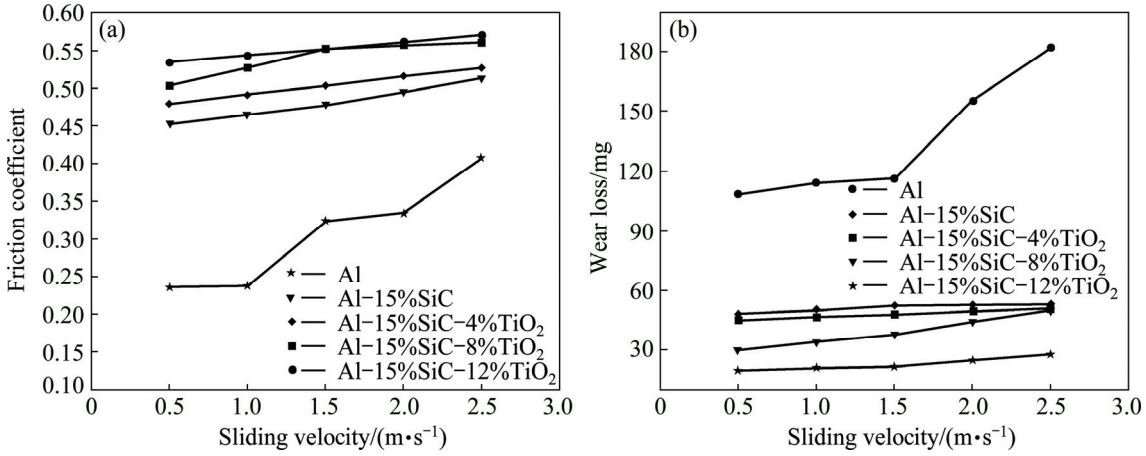

Fig. 6 Effect of sliding velocity on friction coefficient (a) and wear loss (b) of Al hybrid composites

leads to the formation of a protective interface film, which reduces direct contact of sliding faces and wear loss. When the sliding distance reaches higher magnitude, particles are implanted onto the counterface. During subsequent sliding part of the implanted particles are fractured and smeared out from the counter surface. Rest of non-fractured particles abraded the countersurface and increased the wear loss [35−37].

3.7 Interpretation of worn surface

SEM images of worn surfaces of Al matrix, hybridized and non-hybridized composites are shown in Figs. 8−12. Deep plastic grooves and craters are found on the worn surface of Al matrix (Fig. 8(b)). During the sliding wear, due to high plastic deformation, subsurface cracking takes place, which results in particle pullout. The pulled out particles develop craters on the sliding surface of Al performs [38]. Adhesion of flat debris is also apparent from Fig. 8(a), suggesting delamination wear. Worn surface of Al−15%SiC composites (Fig. 9) shows the presence of wear scars adhered to the sliding surface which can be due to compaction of particles underneath the counterface [39]. It is observed that high plastic flow increases the shear stress required to peel off the wearing surface and encourages delamination wear mechanism [40].

Figure 10 shows the wear pattern of Al−15%SiC−4%TiO_2 hybrid composites. The micrographs clearly show the formation of a thin adhesive layer on the worn surface. From Fig. 10(a), it is understood that, high plastic strain induced leads to shear instability of the particles, which is indicated by the distribution of loose fragments of oxide scars [28,40]. The worn surface also shows fractured particles of reinforcements and the matrix, which promotes more loss of materials (Fig. 10(b)). The shallow grooves evident from the micrograph (Fig. 10(a)) also support abrasive wear mechanism [40,41].

Figure 11 reports the wear configuration of the composite preforms reinforced with 8% TiO_2. The micrograph displays the existence of minor scratches which can be attributed to superior hardness of TiO_2. The availability of loose fragments of oxide debris indicates fretting wear due to the cyclic stress developed during the sliding of mating surfaces.

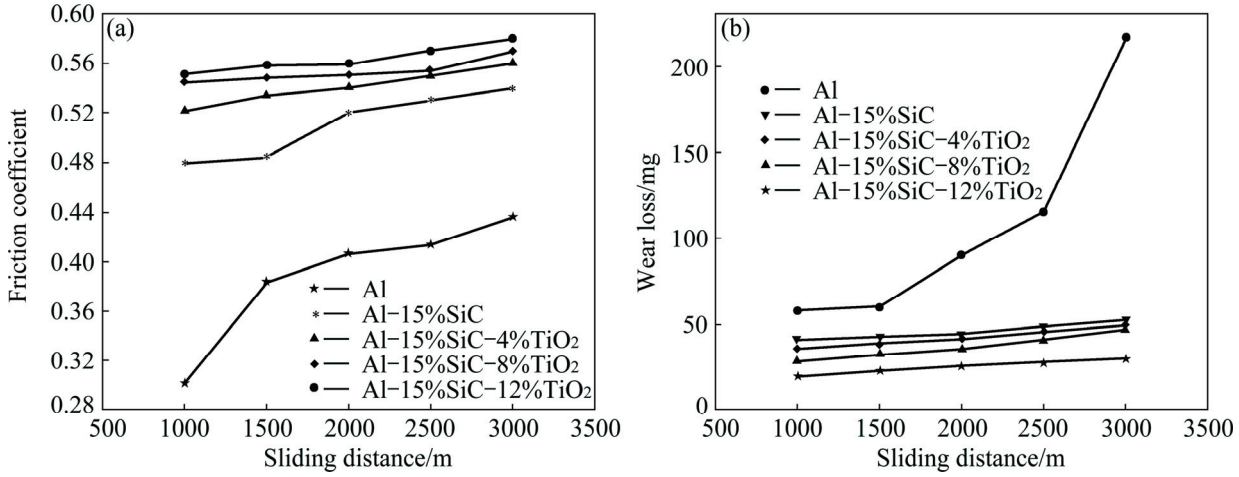

Fig. 7 Effect of sliding distance on friction coefficient (a) and wear loss (b) of Al hybrid composites

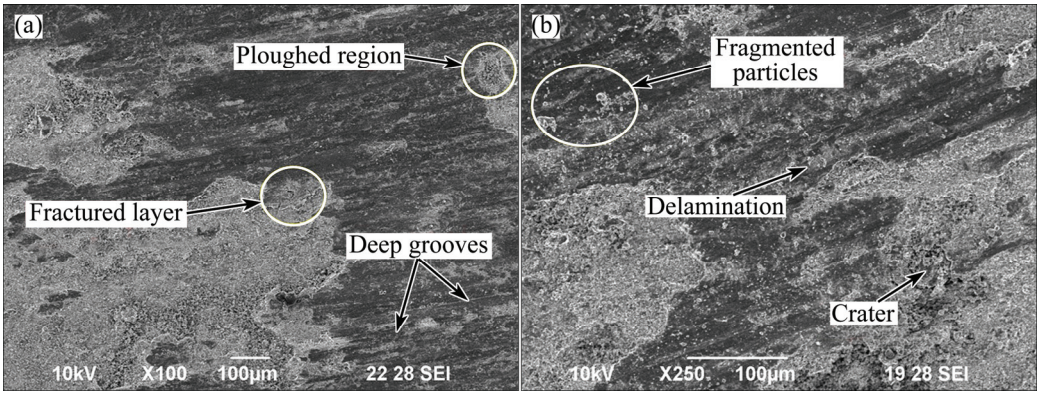

Fig. 8 SEM images of worn surface of Al matrix at applied load of 60 N, sliding velocity of 2.5 m/s and sliding distance of 3000 m: (a) Low magnification; (b) High magnification

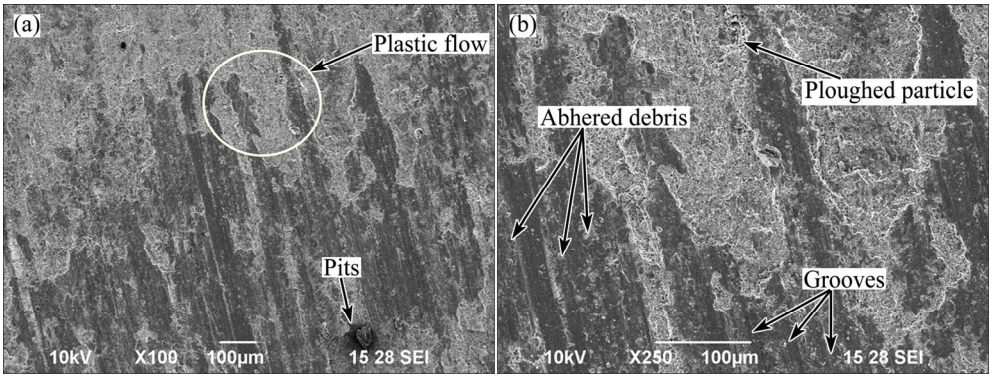

Fig. 9 SEM images of worn surface of Al−15%SiC composite at applied load of 60 N, sliding velocity of 2.5 m/s and sliding distance of 3000 m: (a) Low magnification; (b) High magnification

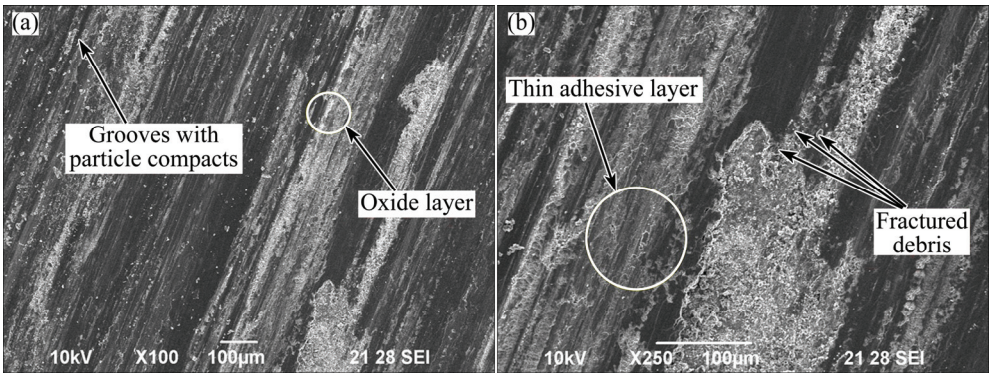

Fig. 10 SEM images of worn surface of Al−15%SiC−4%TiO_2 hybrid composite at applied load of 60 N, sliding velocity of 2.5 m/s and sliding distance of 3000 m: (a) Low magnification; (b) High magnification

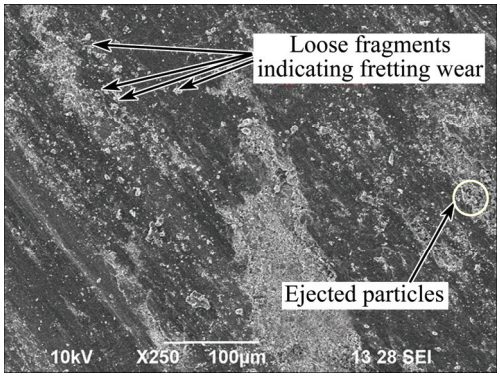

Fig. 11 SEM image of worn surface of Al−15%SiC−8%TiO_2 hybrid composite at applied load of 60 N, sliding velocity of 2.5 m/s and sliding distance of 3000 m

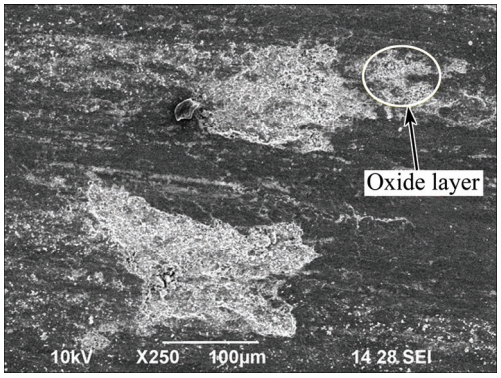

Fig. 12 SEM image of Al−15%SiC−12%TiO_2 hybrid composite at applied load of 60 N, sliding velocity of 2.5 m/s and sliding distance of 3000 m

Hybrid composites reinforced with Al−15%SiC−12%TiO_2 unveil low wear loss which is indicated by the restriction of grooves along the worn surface (Fig. 12). Restriction of grooves along the sliding surface can be attributed to the high dislocation density of the deformed planes and high content of TiO_2 (12%). The presence of TiO_2 offers extreme hardness to the composites and reduces loss of material. Evidence of the oxide layer and the adhesive compacted particles on the worn surface obviously restricts severe plastic deformation thereby lowers the wear loss [42]. The examination of the wear pattern thus noticeably dictates adhesive wear mechanism. Table 3 sums up the wear mechanisms identified for the corresponding material.

Figure 13 shows the EDS patterns of TiO_2 reinforced composites. The presence of oxides in the respective composites is evident from the patterns. EDS patterns depict the existence of considerable amount of oxygen on the worn surface which also shows increasing trend with the content of TiO_2. Oxidation occurs due to the generation of frictional heat during sliding of surfaces. The protective oxide layer minimizes the

Table 3 Summary of worn surface interpretations

Sample No.	Composition/%	Wear mechanism identified
1	Al	Delamination wear
2	Al−15%SiC composite	Delamination & adhesive wear
3	Al−15%SiC−4%TiO_2 hybrid composite	Abrasive wear
4	Al−15%SiC−8%TiO_2 hybrid composite	Fretting wear
5	Al−15%SiC−12%TiO_2 hybrid composite	Adhesive wear

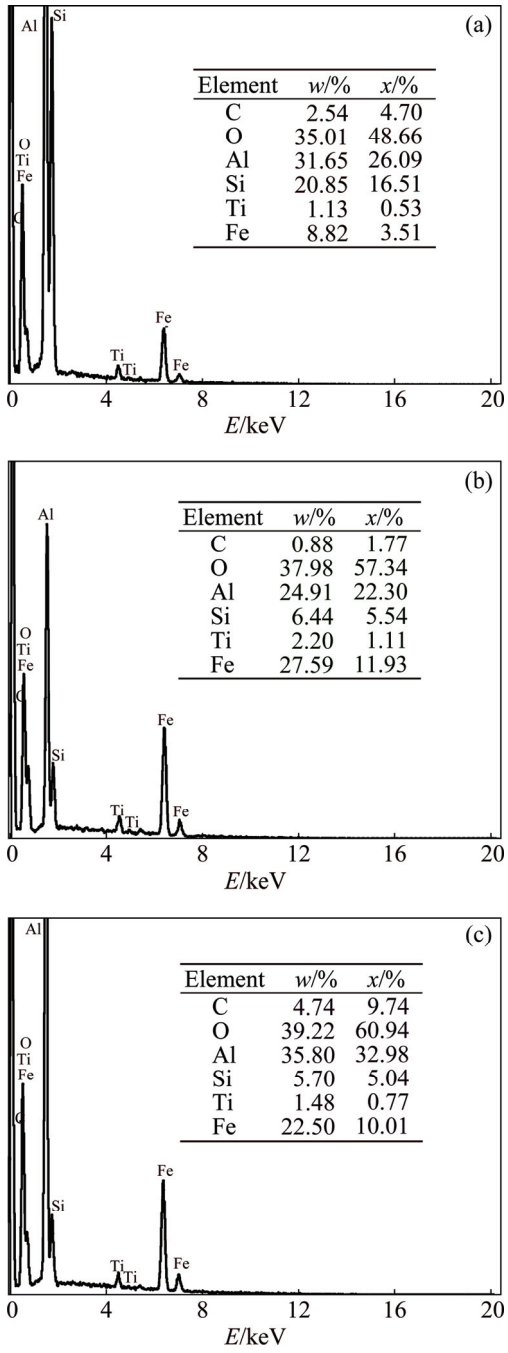

Fig. 13 EDS patterns of worn surfaces of Al−SiC−4%TiO_2 (a), Al−SiC−8%TiO_2 (b), Al−SiC−12%TiO_2 (c) composites

effective area of contact between the mating surfaces thereby lowers the wear loss [42].

3.8 Examination of wear debris

The examination of the wear debris using SEM images obviously indicates the mechanism of wear. Figures 14(a)−(e) display the micrographs of fragments of particles from the worn surface of pure Al matrix, non-hybridized Al−SiC and the hybridized Al−SiC−TiO_2 composites.

The wear debris shown in Fig. 14(a) confirms the presence of thin sheet like Al particles. Formation of thin Al sheets indicates severe plastic deformation and concludes delamination wear. It is recognizable from Fig. 14(b) that during sliding, the wear debris obtained from Al−15%SiC composites consists of particles with thin adhered fragments. The micrograph also shows debris with reduced mean size due to the presence of hard SiC phase in the matrix.

The wear debris of hybrid composites reinforced with 4% TiO_2 consists of a combination of thin sheets and fine loose particles (Fig. 14(c)). The presence of deep grooved sheets is also apparent from the micrograph, indicating delamination wear mechanism. Figure 14(d) shows the fragments of particles obtained from the worn surface of Al−15%SiC−8%TiO_2 hybrid composites. The SEM image also perceives that the increase in TiO_2 content from 4% to 8% apparently reduces the mean size of wear debris. Furthermore, the SEM image also shows minimum quantity of particulate fragments. Existence of loose fragments may be due to micro machining of particles during sliding wear. Wear debris collected for hybrid composites reinforced with 12% TiO_2 is presented in Fig. 14(e). The micrograph clearly displays particles of uniform size in a minimum count. The presence of TiO_2 in the composite increases the dislocation density and minimizes the plastic deformation. Thus, the hardness of the sliding surface increases and the size of the particles is reduced. It is therefore confirmed that the amount of hard phases like SiC and TiO_2 dictates the size and morphology of wear debris [42].

Figure 15 displays the XRD patterns of the wear debris collected for the proposed composites. Figure 15(a) shows the configuration of the wear debris obtained for Al−15%SiC composites during the sliding wear. The XRD pattern shows the peaks representing the presence of oxide compounds. During sliding, three body abrasions of the hard reinforcement phase remove the protective oxide layer formed on the worn surface and those removed layers mix with the fragments as debris [37]. The XRD pattern of 4%TiO_2 hybrid composite shown in Fig. 15(b) also reveals the presence of Al, SiC and TiO_2 phases. The presence of titanium carbide (TiC)

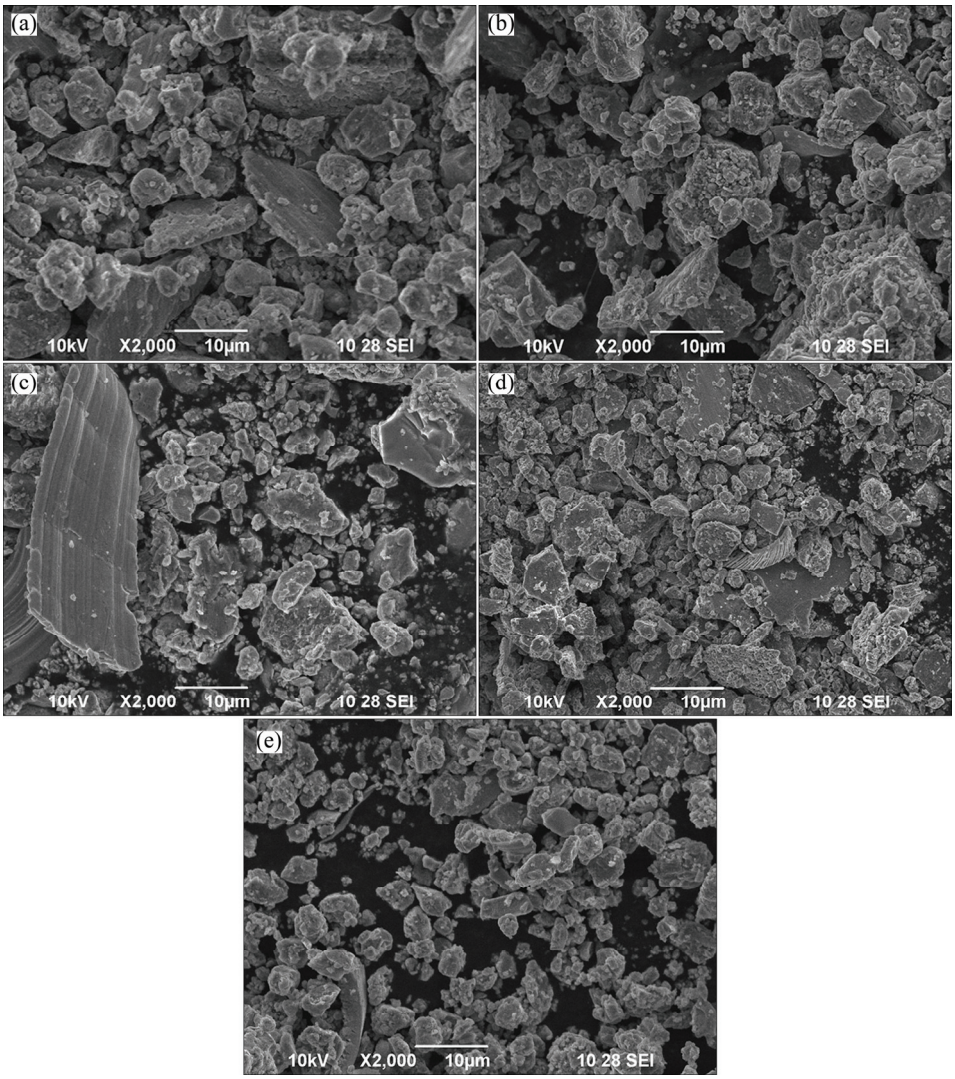

Fig. 14 SEM images of wear debris collected from worn surface of pure Al (a), Al−15%SiC (b), Al−15%SiC−4%TiO_2 (c), Al−15%SiC−8%TiO_2 (d) and Al−15%SiC−12% TiO_2 (e)

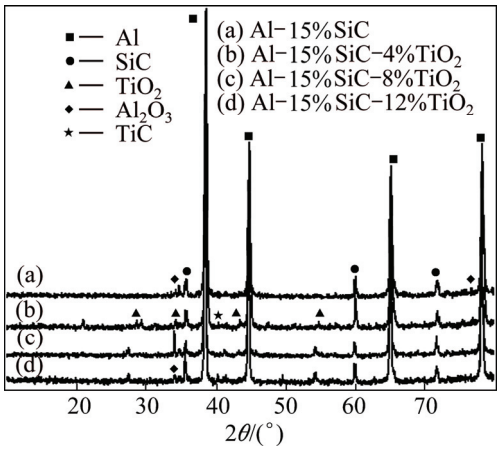

Fig. 15 XRD patterns of wear debris collected from worn surface of proposed composites

in the wear debris of 4% TiO_2 increases the brittleness of the material which brings down the shear strain on the sliding surface and results in higher wear rate. In the case of wear debris obtained for 8% TiO_2 and 12% TiO_2 hybrid composites, minimum oxide phases are present as evident from Figs. 15(c) and (d). Minimum oxide phases specify prevention of micro machining of particles by the reinforcement phase and less plastic deformation of the material, which lead to low wear loss.

4 Conclusions

1) The natural mineral rutile (TiO_2) was reinforced to Al−15%SiC composites through powder metallurgy process. Inclusion of rutile increases the density and microhardness of the hybrid composites. The density and microhardness show remarkable improvement with the mass fraction of TiO_2 (rutile).

2) The wear study made on the proposed composites discloses that the Al−SiC−TiO_2 hybrid composites display better wear resistance than the unreinforced Al−SiC composites and the base matrix.

Subsequently, an increase in the content of TiO_2 (rutile) shows low wear loss. Thus, Al−15%SiC reinforced with 12% TiO_2 will be the better candidate material for high wear resistance.

3) From the SEM image, it was observed that delamination and adhesive wear are the predominant wear mechanisms. Fragmented wear debris dictates micro cutting of the particles during the sliding wear.

4) The micrograph of the wear debris collected for the hybrid composites shows reduced mean size as the content of TiO_2 (rutile) increases.

5) XRD patterns of wear debris reveal the presence of minimum oxide phases specifically for composites reinforced with 12% TiO_2. Minimum oxide phases indicate prevention of micro machining of particles by the reinforcement phase and less plastic deformation of the material, which led to low wear loss.

6) The micrographs and XRD patterns clearly indicate that rutile is dominant in enhancing the wear and micro hardness properties of the proposed composite material.

Acknowledgement

The authors are grateful to the Centre for Research in Metallurgy, School of Mechanical Sciences, Karunya University, Coimbatore, India and Department of Physics, Manonmaniam Sundaranar University, Tirunelveli, Tamilnadu, India for rendering their facilities. One of the authors, Mr. C. Antony Vasantha Kumar aspires to acknowledge Mr. A. RAJA and Mr. I. DEVAMANOHARAN (Central Research Facilities, Karunya University) for their support towards successful completion of this work. The corresponding author also wish to acknowledge Mr. GOWTHAM (SCAD College of Engineering & Technology, Tirunelveli, Tamilnadu, India) for his assistance during the progress of this work.

References

[1] SONG Min. Effects of volume fraction of SiC particles on mechanical properties of SiC/Al composites [J]. Transactions of Nonferrous Metals Society of China, 2009, 19(6): 1400−1404.

[2] NATARAJAN N, VIJAYARANGAN S, RAJENDRAN I. Wear behaviour of A356/25 SiC_P aluminium matrix composites sliding against automobile friction material [J]. Wear, 2006, 261: 812−822.

[3] IIZUKA T, OUYANG Qiu-bao. Microstructures and mechanical properties of $MgAl_2O_4$ particle-reinforced AC4C aluminum composites [J]. Transactions of Nonferrous Metals Society of China, 2014, 24(7): 2337−2345.

[4] RAGUWANSHI N K R, AJAY P, MANDLOI R. Failure analysis of internal combustion engine valves: A review [J]. International Journal of Innovative Research in Science Engineering and Technology, 2012, 1(2): 173−181.

[5] BELETE S Y, JHA P K, MAHAPATRA M M. Effect of sliding distance, applied load and wt % of reinforcement on the abrasive wear properties of in-situ synthesized Al−12%Si/TiC composites [J]. Tribology Transactions, 2013, 56 (4): 546−554.

[6] BELETE S Y, JHA P K, MAHAPATRA M M. On modeling the abrasive wear characteristics of in situ Al−12%Si/TiC composites [J]. Materials and Design, 2013, 50: 277−284.

[7] CANDAN E, AHLATCI H, CIMENOGLU H. Abrasive wear behaviour of Al−SiC composites produced by pressure infiltration technique [J]. Wear, 2001, 247: 133−138.

[8] BASAVARAJAPPA S, CHANDRAMOHAN G, ARJUN M, MUKUNDAN T, SUBRAMANIAN R, GOPALAKRISHNAN P. Influence of sliding speed on the dry sliding wear behaviour and the subsurface deformation on hybrid metal matrix composite [J]. Wear, 2007, 262: 1007−1012.

[9] VEERESH KUMAR G B, RAO C S P, SELVARAJ N. Studies on mechanical and dry sliding wear of Al6061−SiC composites [J]. Composites Part B, 2012, 43: 1185−1191.

[10] SUN Zhi-qiang, ZHANG Di, LI Guo-bin. Evaluation of dry sliding wear behaviour of silicon particles reinforced aluminium matrix composites [J]. Materials and Design, 2005, 26: 454−458.

[11] LIU Z Y, WANG Q Z, XIAO B L, MA Z Y, LIU Y. Experimental and modelling investigation on SiC_P distribution in powder metallurgy processed SiC_P/2024 Al composites [J]. Materials Science and Engineering A, 2010, 527: 5582−5591.

[12] ADEL MAHAMOOD H, AHMAD TURKI M, ABDALLA A, MOHAMMED T H. Wear behaviour of Al−Cu and Al−Cu/SiC components produced by powder metallurgy [J]. Journal of Materials Science, 2008, 43: 5368−5375.

[13] SAHIN Y, KILICLI V. Abrasive wear behaviour of SiC_P/Al alloy composite in comparison with ausferritic ductile iron [J]. Wear, 2011, 271: 2766−2774.

[14] BASAVARAJAPPA S, CHANDRAMOHAN G, SUBRAMANIAN R, CHANDRASEKAR A. Dry sliding wear behaviour of Al 2219/SiC metal matrix composites [J]. Material Science Poland, 2006, 24: 357−366.

[15] SUN Chao, SONG Min, WANG Zhang-wei, HE Yue-hui. Effect of particle size on the microstructures and mechanical properties of SiC- reinforced pure Aluminium composites [J]. Journal of Materials Engineering and Performance, 2011, 20: 1606−1612.

[16] CERIT A A, KARAMIS M B, NAIR F, YILDIZLI K. Effect of reinforcement particle size and volume fraction on wear behaviour of Metal matrix composites [J]. Tribology in Industry, 2008, 30 (3−4): 31−36.

[17] GOO B C, KIM M H. Characteristics of A356/SiC_P and A390/SiC_P composites [J]. Journal of Mechanical Science and Technology, 2012, 26(7): 2097−2100.

[18] SANKAR M, DILIP KUMAR M, GOPA M, ROY G S, DEBADHAYAN B, MANTRY S, SINGH S K. A study on sintered TiO_2 and TiO_2/SiC composites synthesized through chemical reaction based solution method [J]. Journal of Composite Materials, 2013, 47 (24): 3081−3089.

[19] RAMA A, KUMAR S, GURMEL S, PANDEY O P. Influence of particle size and temperature on the wear properties of rutile-reinforced aluminium metal matrix composite [J]. Journal of Composite Materials, 2014, doi: 10.1177/0021998314526079.

[20] RAMESH C S, ANWAR KHAN A R, RAVIKUMAR N, SAVANPRABHU P. Prediction of wear coefficient of Al6061−TiO_2 composites [J]. Wear, 2005, 259: 602−608.

[21] CHAUDHURY S K, SINGH A K, SIVARAMAKRISHNAN C S S, PANIGRAHI S. Preparation and thermo mechanical properties of stir cast Al−2Mg−11TiO_2 (rutile) composite [J]. Bulletin of Materials Science, 2004, 27(6): 517−521.

[22] TROMANS D, MEECH J A. Fracture toughness and surface energies of minerals: Theoretical estimates for oxides, sulphides, silicates and halides [J]. Minerals Engineering, 2002, 15: 1027−1041.

[23] FATHY A, EL-KADY O, MOHAMMED M M M. Effect of iron addition on microstructure, mechanical and magnetic properties of

Al-matrix composite produced by powder metallurgy route [J]. Transactions of Nonferrous Metals Society of China, 2015, 25(1): 46−53.

[24] BIROL Y. Synthesis of Al−SrB_6 composite via powder metallurgy processing [J]. Transactions of Nonferrous Metals Society of China, 2015, 25(3): 677−682.

[25] LIU Pei, WANG Ai-qin, XIE Jing-pei, HAO Shi-ming. Characterization and evaluation of interface in SiC_p/2024 Al composite [J]. Transactions of Nonferrous Metals Society of China, 2015, 25(5): 1410−1418.

[26] YUSUF S. Abrasive wear behaviour of SiC/2014 aluminium composite [J]. Tribology International, 2010, 43: 939−943.

[27] WANG Yi-qi, SONG Jung-il. Dry sliding wear behaviour of Al_2O_3 fiber and SiC particle reinforced aluminium based MMCs fabricated by squeeze casting method [J]. Transactions of Nonferrous Metals Society of China, 2011, 21(7): 1441−1448.

[28] DEUIS R L, SUBRAMANIAN C, YELLUP J M. Dry sliding wear of aluminium composites—A review [J]. Composites Science and Technology, 1997, 57: 415−435.

[29] RAMESH C S, BHARATHESH T P, VERMA S M, KESHAVAMURTHY R. Sand abrasive wear behavior of hot forges Al 6061−TiO_2 composites [J]. Journal of Materials Engineering and Performance, 2012, 21: 74−82.

[30] JIANG Xiao-song, WANG Nai-juan, ZHU De-gui. Friction and wear properties of in-situ synthesized Al_2O_3 reinforced aluminum composites [J]. Transactions of Nonferrous Metals Society of China, 2014, 24(7): 2352−2358.

[31] AL-QUTUB A M, ALAM I M, ABDUL SAMAD M A. Wear and friction of Al−$A1_20_3$ composites at various sliding speeds [J]. Journal of Materials Science, 2008, 43: 5797−5803.

[32] KUMAR S, BALASUBRAMANIAN V. Effect of reinforcement size and volume fraction on the abrasive wear behaviour of AA7075 Al/SiC_P P/M composites — A statistical analysis [J]. Tribology International, 2010, 43: 414−422.

[33] SRIVASTAVA V C, RUDRAKSHI G B, UHLENWINKEL V, OJHA S N. Wear characteristics of spray formed Al-alloys and their composites [J]. Journal of Materials Science, 2009, 44: 2288−2299.

[34] ALIDOKHT S A, ABDOLLAH-ZADEH A, SOLEYMANI S, ASSADI H. Microstructure and tribological performance of an aluminium alloy based hybrid composite produced by friction stir processing [J]. Materials and Design, 2011, 32: 2727−2733.

[35] KUMAR S, BALASUBRAMANIAN V. Developing a mathematical model to evaluate wear rate of AA 7075/SiC_P powder metallurgy composites [J]. Wear, 2008, 264: 1026−1034.

[36] WANG D Z, PENG H X, LIU J, YAO C K. Wear behaviour and micro structural changes of SiC_W–Al composite under unlubricated sliding friction [J]. Wear, 1995, 184: 187−192.

[37] JIN Pei-peng, CHEN Geng, HAN Li, WANG Jin-Hui. Dry sliding friction and wear behaviors of $Mg_2B_2O_5$ whisker reinforced 6061Al matrix composites [J]. Transactions of Nonferrous Metals Society of China, 2014, 24(1): 49−57.

[38] DINAHARAN I, MURUGAN N. Dry sliding wear behaviour of AA6061/ZrB_2 in-situ composite [J]. Transactions of Nonferrous Metals Society of China, 2012, 22: 810−818.

[39] KARAMIS M B, ALPER CERIT A, BURHAN SELCUK, FEHMI NAIR. The effects of different ceramics size and volume fraction on wear behaviour of Al matrix composites (for automobile cam materials) [J]. Wear, 2012, 289: 73−81.

[40] ASHOK KUMAR B, MURUGAN N, DINAHARAN I. Dry sliding wear behavior of stir cast AA6061-T6/AlNp composite [J]. Transactions of Nonferrous Metals Society of China, 2014, 24(9): 2785−2795.

[41] HABIBOLAHZADEH A, HASSANI A, BAGHERPOUR E, TAHERI M. Dry friction and wear behavior of in-situ Al/Al3Ti composite [J]. Journal of Composite Materials, 2014, 48(9): 1049−1059.

[42] RAVINDRAN P, MANISEKAR K, RATHIKA P, NARAYANASAMY P. Tribological properties of powder metallurgy –Processed aluminium self-lubricating hybrid composites with SiC additions [J]. Materials and Design, 2013, 45: 561−570.

锐钛矿(TiO_2)含量对粉末冶金制备铝基复合材料磨损性能和显微硬度的影响

C. ANTONY VASANTHA KUMAR[1], J. SELWIN RAJADURAI[2]

1. Department of Mechanical Engineering, Scad College of Engineering and Technology, Cheranmahadevi, Tirunelveli 627414, Tamilnadu, India;
2. Department of Mechanical Engineering, Government College of Engineering, Tirunelveli 627007, Tamilnadu, India

摘　要：研究了锐钛矿(TiO_2)含量对铝基复合材料磨损性能和显微硬度的影响。采用粉末冶金方法制备不同 TiO_2 含量(0，4%，8%，12%，质量分数)的 Al−15%SiC 复合材料。在干摩擦条件下，采用盘−销装置进行磨损试验。采用 X 射线衍射仪、扫描电子显微镜(SEM)和能谱仪(EDS)对预制品进行表征。复合材料的光学显微组织表明 TiO_2 在基体中分布均匀。定量分析表明，随着 TiO_2 含量的增加，复合材料的抗磨损性能和显微硬度提高。SEM 显微组织揭示了复合材料的高抗磨损性能与变形面的高位错密度和 TiO_2 的高硬度有关。磨屑的 SEM 组织表明随着 TiO_2 含量的增加，磨屑的尺寸逐渐减小。能谱分析证实氧化层的形成能明显地减小摩擦表面的有效接触面积，进而减小复合材料的磨损。分层和黏附磨损是主要的磨损机理。

关键词：铝；金属基复合材料；锐钛矿；粉末冶金；滑动磨损

(Edited by Yun-bin HE)